A Model for Toughening of Semicrystalline Polymers

Laurent Corté*,† and Ludwik Leibler

Matière Molle et Chimie, Ecole Supérieure de Physique Chimie Industrielle (UMR ESPCI−CNRS 7167), 10 rue Vauquelin 75231 Paris Cedex 05, France

Received March 21, 2007; Revised Manuscript Received May 21, 2007

ABSTRACT: Dispersing particles within a semicrystalline polymer can result in remarkable impact strength improvement and opens promising routes toward super-tough materials. Although the technique is extensively employed to modify polymer properties, predicting which dispersions yield toughness remains a challenging issue. By comparing the characteristic lengths and deformation processes involved in toughening, we explain why a minimum matrix confinement or ligament thickness is required to induce ductility. Our model was used to interpret experimental data and show how this critical confinement length depends on material properties, temperature, and processing history. Most importantly, it reveals an unexpected particle size effect. The predictions provide fresh insight into the design of toughened materials. The model also provides guidance to understanding the fracture mechanics of other complex systems such as composites or biological matter.

Introduction

Most solids are heterogeneous materials. Among plastics, semicrystalline polymers exhibit remarkably complex structures at the molecular scale.[1] During processing, these macromolecular chains spontaneously fold and form dense crystalline lamellae separated by amorphous regions, as depicted in Figure 1a. Because of the high density and melting point of these lamellae, semicrystalline polymers such as polyamides, polyolefins, or cellulose exhibit excellent chemical resistance and can maintain physical integrity at temperatures exceeding 100 °C. These characteristics make them attractive to many applications ranging from tubing to components for aeronautics. Unfortunately, these materials are generally prone to ductile failure and are known to become brittle at low temperature and in the presence of notches that concentrate stress. A major discovery was that particle inclusion in the polymer matrix can significantly relax the strong stresses developed in front of notches and impart ductility, especially at low temperature.[2−4] This toughening strategy, together with recent developments in polymer science, has increased the impact strength of semicrystalline polymers by an order of magnitude and opened promising routes toward new super-tough and rigid materials.[5−7] Yet, the toughening ability of dispersions remains largely unpredictable and is usually probed by costly trial-and-error experiments.

We show here that a microscopic model of the fracture mechanism captures the existence of a minimum confinement length governing the onset of ductility. The analysis also explains how toughening depends on the matrix and dispersion characteristics as well as on the impact conditions. This generic picture could lead toward an understanding of the fracture and confinement effect in other composite materials such as botanical structures made of highly flawed cellulose-based tissues.[8]

Numerous studies[9−12] initiated by the first observations of Wu[13] have shown that a minimum confinement of the polymer matrix is necessary to induce ductility. This confinement is usually characterized by the average surface-to-surface distance between particles, L, which is also referred to as the average matrix ligament thickness. For given impact conditions, Wu found that toughening can only be achieved below some critical ligament thickness, L_c (Figure 1b). This critical length is commonly considered as an intrinsic property of the matrix, independent of the size and nature of the particles. For example, standard impact conditions yield a value of about 0.3 μm for L_c in polyamide-66,[13] while it is about 2 μm in polyamide-12.[14] Shedding some light on this intriguing length scale is the purpose of this paper.

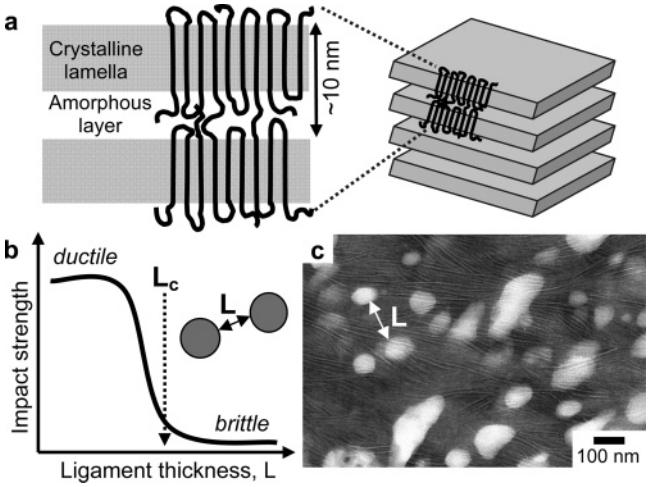

Figure 1. (a) Schematic representation of the molecular organization of semicrystalline polymers. **(b)** Typical evolution of the impact strength of toughened semicrystalline polymers as a function of average ligament thickness L. **(c)** Transmission electron micrograph taken from an injected impact test sample of polyamide-12 filled with rubber particles. Rubber particles appear in white. A specific staining of the matrix reveals bright crystalline lamellae separated by dark amorphous regions. Crystalline lamellae exhibit a long-range orientation perpendicular to the local flow undergone during processing.[14]

Initial attempts to explain the origin of L_c were based on continuous media mechanics and inevitably failed to capture the existence of a critical length governing toughening.[15,16] Indeed, dimensional considerations suggest that a geometrical description of the dispersion is insufficient and that L_c should be related to some other characteristic length of toughened materials. A microscopic model proposed by Argon et al.[17] first introduced the concept that L_c corresponds to a characteristic

* Corresponding author. E-mail : corte@nyu.edu.
† Present address: Center for Soft Matter Research, New York University, New York, NY 10003.

10.1021/ma0706935 CCC: $37.00
Published on Web 06/30/2007

length of the semicrystalline matrix. Their research suggested that during matrix crystallization crystalline lamellae grow perpendicularly to the particle surface and form radially oriented layers, the thickness of which depends on matrix properties. Ductility is thus achieved when these oriented layers percolate through the whole material and provide a path where plastic deformation propagates and dissipates impact energy.

The oriented layer model has been challenged by several experimental observations. In particular, it was found that L_c increases linearly with impact temperature.[9] Yet, the percolation of oriented layers should be a definitive property of a toughened system once the matrix has crystallized. Moreover, recent microscopic observations[14,18] suggest that crystalline lamellae do not form oriented layers but that their orientation is rather strongly determined by the local flows and thermal history undergone during processing, as illustrated by the TEM micrograph given in Figure 1c.

We propose a new description of toughening that considers both delocalized and localized deformation processes; specifically, a shear yielding process which allows ductile failure as opposed to the opening and coalescence of cracks which causes brittle fracture. Since the pioneering work of Griffith,[19] the latter mechanism is known to initiate the brittle fracture of most heterogeneous media.[20] In the case of semicrystalline polymers, seminal X-ray studies by Kuksenko and Tamusz[21] showed that micron- or submicron-sized cracks accumulate in semicrystalline specimens and coalesce in avalanche at some critical crack concentration, therefore causing a brittle fracture. We compare this brittle mechanism to the shear yielding of the matrix initiated around impact filler particles and show how ductility is achieved below a critical ligament thickness that depends on matrix properties, particle size, and impact conditions.

Model

Fracture of the Semicrystalline Matrix. We begin with a description of the fracture processes and mechanisms of the neat semicrystalline matrix with no added particles. Kuksenko and Tamusz[21] studied semicrystalline polymers under load using X-ray scattering. Their observations revealed that a great number of micron- or submicron-sized cracks open in poorly cohesive amorphous layers and accumulate in semicrystalline specimens long before their final rupture. Eventually, a brittle fracture occurs when these cracks coalesce in avalanche at some critical concentration denoted as ρ^*. For processed semicrystalline polymers, ρ^* is typically of the order of $10^{14}-10^{16}$ cm^{-3}. Interestingly, this critical concentration shows the existence of a critical distance between cracks ξ^* given by $\rho^{*-1/3}$, which is thus of the order of 100 nm.

These X-ray measurements further reveal that the crack dimensions vary little with the load and that ξ^* is always comparable to the crack size. Such a scaling points out that coalescence is driven by the local stress fields around cracks, which are shown to extend over distances commensurable with the crack size.[22] As a result, two coalescing cracks form a larger crack that interacts further. If several cracks had already accumulated in the specimen, this larger crack immediately coalesces with other neighboring cracks and triggers the avalanche process that leads to brittle fracture.

The formation of these cracks has been shown to depend on the molecular organization in the amorphous regions and on the scission of tie chains bridging crystalline lamellae.[21,23] However, the question of what sets the characteristic size of microcracks is unclear and difficult to investigate experimentally. Lacking a clear molecular description, brittle fracture is usually characterized by macroscopic measurements at high speed and low temperature.[24] In the following analysis, we assume that the critical crack concentration is reached when the largest normal stress attains the characteristic value σ_B. This criterion for brittle fracture is given by $\mathrm{Max}(\sigma_i) = \sigma_B$ ($i \in \{1,2,3\}$), where σ_B is the tensile stress at break and σ_1, σ_2, and σ_3 are the normal principal stresses which are depicted in Figure 2 along axis 1, 2, and 3 for the sake of simplicity. A different stress criterion based on hydrostatic stress for instance would lead here to similar conclusions.

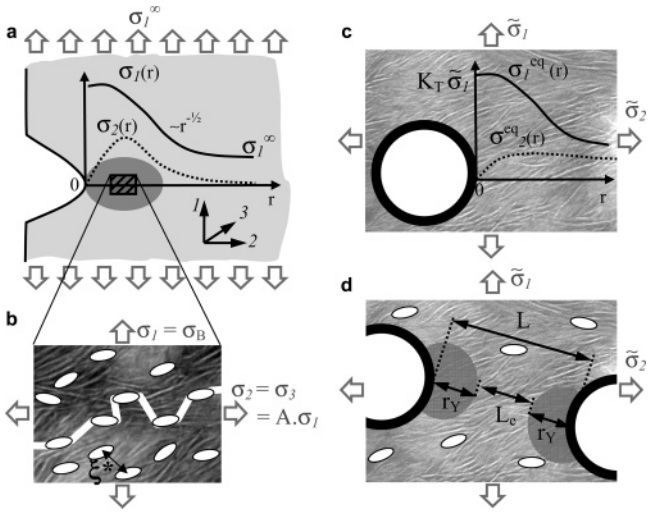

Figure 2. (a) Stress distribution in front of a notch submitted to a remote tensile stress σ_1^∞. Curves illustrate the typical stress profiles for stress components σ_1 and σ_2 in the plane of the notch as a function of the distance r from the notch tip. A gray region represent the process zone ahead of the notch. **(**b**)** Stress state in the process zone where triaxial stresses are the greatest. White ellipsoids superimposed to the TEM micrograph illustrate cracks opening between crystalline lamellae. The thick white line represents the catastrophic coalescence occurring when $\sigma_1 = \sigma_B$ if the critical distance between cracks ξ^* is reached before initiation of shear yielding. **(**c**)** Local stress distribution around voided particles. Curves represent the profiles for stress component σ_1^{eq} and σ_2^{eq} in the equatorial plane of the particle as a function of the distance r from the particle surface. **(**d**)** Schematic representation of the deformation processes in toughened systems: yielded regions (in dark gray) grow around particles while cracks open in the elastic matrix far from the particles.

As opposed to brittle fracture and crack opening, a tough and ductile behavior is usually obtained at high temperature, low impact speed, or low stress triaxiality. In these conditions, the mobility of polymer chains is sufficient to allow chain displacements in the crystalline lamellae. These displacements are activated when shear stresses reach a critical yield value at which chains slip along each other. Above this yield point, the initial crystalline organization breaks and re-forms into highly elongated fibrils.[25] This ductile process generates significant chain friction, which dissipates impact energy, stabilizes crack propagation, and yields high values of impact strength. We describe the onset of this shear yielding deformation using a Tresca criterion given by $\mathrm{Max}(|\sigma_i - \sigma_j|) = \sigma_Y$ ($i, j \in \{1,2,3\}$) where σ_Y is the macroscopic tensile yield stress.

Most data on the fracture of semicrystalline polymers are collected with standard Charpy or Izod techniques for which a notched test bar having well-defined dimensions is impacted by a pendulum at a controlled speed and temperature. At the beginning of impact, the test bar bends as it is pushed by the pendulum and tensile stresses apply normal to the notch. In Figure 2a, these tensile stresses are denoted σ_1^∞ and apply along axis 1. Because these tensile stresses cannot be transmitted

close to the free faces of the notch, they are concentrated and redistributed in all directions ahead of the notch tip. Asymptotically, both this stress concentration and triaxiality decay with the distance r from the notch tip as $r^{-1/2}$. As the pendulum pushes the test bar further, σ_1^∞ increases and damage accumulates in a process zone located at the front of the notch tip.

Ultimately, the brittle or ductile failure of the sample depends upon which deformation mechanism prevails in a region of the process zone where stress triaxiality is highest. Figure 2b illustrates the local stress state in this key region where σ_1 is the amplified tensile stress along axis 1 ($\sigma_1 > \sigma_1^\infty$). We assume that the global sample geometry is axisymmetric along axis 1 so that the normal stresses, σ_2 and σ_3, in the plane of the notch are equal. In this geometry, the state of stress triaxiality can be quantified using a ratio defined as $A = \sigma_2/\sigma_1 = \sigma_3/\sigma_1$. Depending on the sharpness of the notch, A ranges from 0 for no triaxiality, i.e., no notch, to 1 for maximum triaxiality ($\sigma_1 = \sigma_2 = \sigma_3$). Comparing the criteria for shear yielding and brittle fracture, it appears that the critical crack concentration is attained before shear yielding is initiated if

$$(1 - A)\sigma_B < \sigma_Y \tag{1}$$

In this case, an unstable crack is most likely to propagate through the whole sample causing its brittle failure (Figure 2b). In the usual range of temperatures and strain rates, most semicrystalline polymers are ductile in the absence of a notch but become brittle when the sample is notched. In terms of our simple picture, this notch sensitivity implies that both $\sigma_Y < \sigma_B$ and eq 1 are satisfied for some triaxial state of stress characterized by $A > 0$.

Toughening by Dispersing Particles. Consider now a toughened semicrystalline matrix filled with micron-sized spherical particles. In order to predict toughening efficiency, we examine how this particle dispersion can induce a ductile behavior under the triaxial loading conditions described by eq 1 where the neat semicrystalline polymer is brittle. A first requirement for this toughening is for void formation in the particles to relax the triaxial stress state that favors brittle fracture.[5] This is often achieved practically by using soft rubber particles that easily cavitate. More recently, rigid fillers such as $CaCO_3$ particles or clay platelets have been used since they do not induce the stiffness loss obtained with soft rubber fillers.[5,6] For these systems, toughening is achieved when voids are created by debonding at the particle−matrix interface. To first approximation, our toughened system can thus be regarded as a porous material containing a volume fraction Φ of small voids of diameter d.

In the critical process region depicted in Figure 2a, matrix ligaments are subjected to a remote stress field $\tilde{\sigma}$ that depends on the vicinity and geometry of the notch as well as on the presence of voids that reduce the actual load bearing area. The remote stress field as seen by matrix ligaments is denoted by the tilde symbol. It can be estimated from simple stereological considerations[26] and scales as $\tilde{\sigma}_1 \sim K_{notch}(1 - 1.19\Phi^{2/3})^{-1}\sigma_1^\infty$ and $\tilde{\sigma}_2 \sim A\tilde{\sigma}_1$. Here K_{notch} is the concentration factor due to the notch, and $(1 - 1.19\Phi^{2/3})^{-1}$ expresses the stress concentration due to the reduced load bearing area, where Φ is the volume fraction of voids. The local stress distribution within each matrix ligament is also greatly modified by the formation of voids inside the particles, as illustrated in Figure 2c. Normal stresses are amplified in the direction tangential to the particle surface and released in the direction perpendicular to it. Coordinate axes in Figure 2c are chosen along the principal stresses with axis 1 corresponding to the maximum tensile stress. The highest stress concentration occurs at the particle equator. Close to the particle surface, this equatorial stress field is given by $\sigma_1^{eq} = K_T\tilde{\sigma}_1$ and $\sigma_2^{eq} = 0$, where K_T is a stress concentration factor greater than unity. It depends on the particle shape and on the cavitation mechanisms; for example, $K_T = 3$ for an isolated spherical void in an infinite and linearly elastic body.[22]

The relaxation of triaxial stresses surrounding cavitated particles is central to the toughening effect. By suppressing locally the triaxial state of stress, the stress distribution in the vicinity of the particle equator becomes more favorable to the initiation of a shear yielding process. In particular, the size of the region where stress triaxiality is relaxed is of the order of the radius of curvature of the void.[22] Here, a distinction arises between cracks and cavitated particles which are both voids embedded in the semicrystalline matrix. Unlike cavitated particles whose radius of curvature is comparable to their size, cracks are highly elongated and confined between crystalline lamellae. As a result, their radius of curvature at the crack tip should be of the order of the thickness of amorphous layers, which is about 1−10 nm. Stress triaxiality thus relaxes over an extremely small region close to such a sharp tip. Similarly, cracks cannot induce a massive shear yielding even though they can be as large as the rubber particles used for toughening.

When $\tilde{\sigma}_1$ reaches a value of about σ_Y/K_T, the local shear stresses are large enough to initiate matrix yielding near the particle equator. Still, chain slippage cannot be activated in elastic regions further away from the particles where cracks open and accumulate as was the case for the unfilled sample. As the load increases, yielded regions grow around the particles as depicted in Figure 2d. For a given remote stress, the thickness of the elastic ligament L_e is related by

$$L_e(\tilde{\sigma}_1) = L - 2r_Y(\tilde{\sigma}_1) \tag{2}$$

where L is the initial average ligament thickness and $r_Y(\tilde{\sigma}_1)$ the size of yielded regions.

The growth of yielded regions implies a thinning of the elastic areas which support most of the load. This effect is considered implicitly here by renormalizing the remote stress field. A simple but coarse renormalization is to consider that elastic regions carry the entire load. The renormalized remote stress field seen by a matrix ligament would then be given by $\tilde{\sigma}_1 \sim K_{notch}(1 - \alpha(\Phi + \Phi_Y)^{2/3})^{-1}\sigma_1^\infty$, where Φ_Y is the volume fraction of yielded regions and α a geometrical constant characterizing the distribution and shape of voids and yielded regions. From continuum fracture mechanics,[21] we know that $r_Y(\tilde{\sigma}_1)$ scales as $r_Y(\tilde{\sigma}_1) \sim d(K_T\tilde{\sigma}_1/\sigma_Y)^2$ so that the thickness of the elastic ligament $L_e(\tilde{\sigma}_1)$ can be given by

$$L_e(\tilde{\sigma}_1) = L - d\left(\frac{C\tilde{\sigma}_1}{\sigma_Y}\right)^2 \tag{3}$$

Here C is a dimensionless factor that should depend on the ability of particles to release the stress and on the criterion for brittle stress. For instance, choosing a criterion based on the hydrostatic stress for the brittle fracture would yield a factor C scaling as $(1 + 2A)K_T/3$.

We argue that two situations must be distinguished when the critical microcrack concentration is attained in the elastic regions. At this very moment, the thickness of the elastic ligament is given by $L_e(\sigma_B)$ and the mean distance between microcracks is ξ^*.

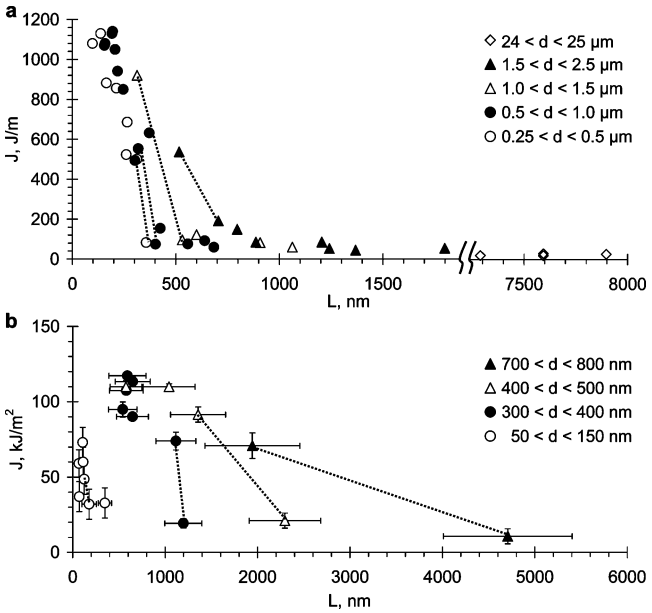

Figure 3. Experimental data showing the impact strength J as a function of ligament thickness L for polyamide-66 **(**a**)** and polyamide-12 **(**b**)** matrices from ref 13 and 27, respectively. Different symbols correspond to different ranges in particle diameter. Dotted lines indicate the position of the brittle-to-ductile transition for each particle size range.

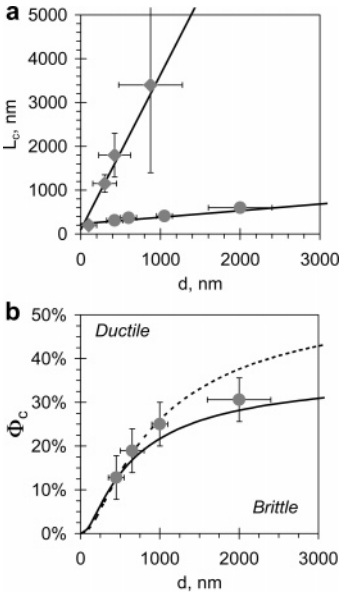

Figure 4. Model predictions for toughened polyamide systems. Symbols show experimental data from the literature for various polyamide matrices. Full lines represent model predictions. **(**a**)** Critical ligament thickness L_c as a function of particle diameter d for polyamide-66 (●) and polyamide-12 (◆) matrices from refs 13 and 27, respectively. Model parameters are $\sigma_Y = 100$ MPa, $\sigma_B = 300$ MPa, $\xi^* = 230$ nm, and $C = 0.11$ for polyamide-66; $\sigma_Y = 70$ MPa, $\sigma_B = 300$ MPa, $\xi^* = 100$ nm, and $C = 0.45$ for polyamide-12. **(**b**)** Critical volume fraction Φ_c as a function of the particle diameter d for polyamide-66 from ref 13. The dashed line corresponds to constant L_c models fixing L_c to 300 nm.

Case i: $L_e(\sigma_B) > \xi^*$. Confinement by yielded regions does not affect microcrack coalescence, and a brittle fracture can still propagate. Though fracture is not ductile, shear yielding around particles might have generated some substantial energy dissipation.

Case ii: $L_e(\sigma_B) < \xi^*$. Confinement by yielded regions is strong enough to shield interactions between microcracks and inhibit their coalescence. Thus, a higher microcrack concentration is required to induce the catastrophic avalanche process. However, experimental observations[21] show that the average distance between microcracks only decreases as $\sigma^{-1/3}$ while the thickness of the elastic matrix ligaments decreases much faster, as σ^2 , as shown in eq 3. As a consequence, a brittle fracture is most unlikely to happen when the elastic ligament is confined below ξ^*.

A critical confinement length appears at the crossover between cases i and ii when $L_e(\sigma_B) = \xi^*$. In other words, toughening is successfully achieved if the initial ligament thickness L is smaller than a critical confinement length L_c given by

$$L_c = \xi^* + d\left(\frac{C\sigma_B}{\sigma_Y}\right)^2 \qquad (4)$$

This equation suggests that L_c depends not only on the matrix characteristics given by ξ^*, σ_B, and σ_Y but also on the particle size d. It is related less obviously to the cavitation process and loading through coefficient C.

Discussion

The particle size dependence predicted by eq 4 is particularly intriguing because L_c is usually considered an intrinsic property of the matrix, i.e., independent of the size and nature of the particles.[10−13] In order to study this paradox, we examined previously reported experimental data for toughened polyamide-66[13] and polyamide-12.[14,27] Measured values of Izod or Charpy impact strength J are reproduced in Figure 3 as a function of ligament thickness L. Different symbols correspond to different ranges in particle size. A linear scale is used here for the abscissa axis (ligament thickness) in order to better reveal the linear dependence on particle size.

For both polyamide-66 and polyamide-12 systems, it is clear that different ranges in particle size exhibit a brittle-to-ductile transition for different ligament thicknesses, therefore confirming the existence of a particle size effect. The linearity of this dependence is better shown in Figure 4a where the critical ligament thickness at the brittle-to-ductile transition is plotted as a function of particle size. Fitting these data with characteristic values for σ_B[28] and σ_Y[29] gives a critical distance ξ^* of the order of 100 nm, which is consistent with the 10−500 nm range measured with X-ray techniques.[21] In nonoriented polyamide-6 samples, Kuksenko and Tamusz find a transverse size of microcracks of about 0.5 μm, as compared to only 10 nm in oriented samples predrawn to a ratio of 4.5. Accordingly, impact test bars obtained by injection molding should have an intermediate coalescence length ξ^* between these two extremes. The coefficient C given by the fits is about 0.1−0.5, which is smaller than the stress concentration factor K_T expected to be greater than 1. Besides probable errors on σ_B and σ_Y, such a low value for C may indicate that cavitated particles still transmit radial stress. As a result, shear yielding would not be as easily activated as it is with perfect voids.

Equation 4 also relates the matrix properties and thus the processing conditions to the critical ligament thickness. In particular, it shows that the particle size dependence varies quadratically with the brittle stress to yield stress ratio, σ_B/σ_Y. This explains why the particle size effect observed in Figures 3 and 4a is much more pronounced in polyamide-12 systems for which $\sigma_Y \sim 70$ MPa than it is in polyamide-66 ones for which $\sigma_Y \sim 100$ MPa. Taking $\sigma_B = 300$ MPa for both polyamide-12 and polyamide-66, this only difference in shear yield stress implies a 2-fold difference in (σ_B/σ_Y).[2] Other

processing effects can be inferred from eq 4 and especially the effect of molecular orientation. Indeed, the shear yield stress,[1,30] the crack size,[21] and more generally the fracture behavior of semicrystalline polymers have been shown to depend significantly on the orientation of the crystalline lamellae. These effects could be introduced in eq 4 using values for σ_Y, σ_B, and ξ^* that vary with the impact direction relative to the orientation of the semicrystalline structure.

The critical confinement criterion expressed by eq 4 can be reformulated in terms of particle size and volume fraction, which are practically easier to handle than the ligament thickness. Assuming a certain particle distribution, L is related to d and Φ by $L = d[(\beta\pi/6\Phi)^{1/3} - 1]$ where β is a geometrical factor close to unity.[13] Substituting this expression in eq 4 gives a minimum volume fraction for the onset of ductility defined by

$$\Phi_c = \frac{\beta\pi}{6}\left(1 + \frac{\xi^*}{d} + \left(\frac{C\sigma_B}{\sigma_Y}\right)^2\right)^{-3} \quad (5)$$

Figure 4b shows the evolution of Φ_c as a function of d for toughened polyamide-66 systems taking $\beta = 1.09$, as it was done in the original study.[13] Our prediction is compared to the dependence that one would obtain with other models such as the oriented layer picture[17] for which L_c is considered to be constant. In Figure 4b, this latter dependence is calculated taking $L_c = 300$ nm, which is commonly adopted for polyamide-66. Both curves exhibit similar trends but differ quantitatively: ductility is more difficult to achieve according to the constant L_c picture. This is explained in terms of microscopic mechanisms: constant L_c models require that shear yielding propagates through the whole ligament thickness to induce ductility. On the contrary, the present model considers a less severe condition for toughening: it is sufficient to confine the matrix below a certain value ξ^* in order to prevent brittle fracture.

Another crucial feature for most applications is to maintain ductility at low impact temperatures. Because temperature and impact speed mostly affect the yield process,[24] their effect can be introduced in the present model through a description of σ_Y. Here we express the dependence of σ_Y on temperature T and strain rate $\dot{\epsilon}$ using a simple linear relation as given by an Eyring description:

$$\sigma_Y(\dot{\epsilon},T) = Y_0 - Y_1(\dot{\epsilon})T \quad (6)$$

where Y_0 and $Y_1(\dot{\epsilon})$ are characteristic parameters of the semicrystalline matrix. Substituting (6) into (5), we derive the temperature of ductile-to-brittle transition T_{DB} as follows:

$$T_{DB} = \frac{Y_0}{Y_1(\dot{\epsilon})} - \frac{C\sigma_B}{Y_1(\dot{\epsilon})}\left[\left(\frac{\beta\pi}{6\Phi}\right)^{1/3} - 1 - \frac{\xi^*}{d}\right]^{-1/2} \quad (7)$$

This expression reveals sharp dependences of T_{DB} with both d (Figure 5a) and Φ (Figure 5b). Figure 5 compares model predictions to experimental data for polyamide-6 systems reported by Borggreve et al.[9] Calculated T_{DB} is obtained with typical values of Y_1 and Y_0 for polyamide-6 in Izod impact conditions.[29] Values obtained for the fitting parameters C and ξ^* are about 0.1−0.3 and 10−100 nm, respectively. In the experimental study, only the weight-average particle size is given, which overestimates the number-average particle size. As a result, the small values obtained here for ξ^* may in reality be larger.

Besides errors coming from Y_0 and Y_1, discrepancies between model and experiment may arise from additional processing effects that are not considered in the initial picture. In particular,

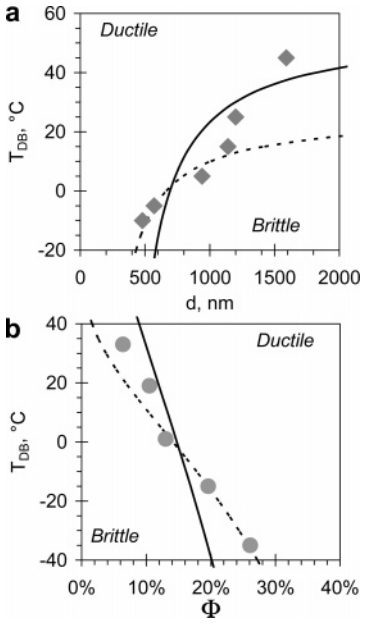

Figure 5. Temperature of ductile-to-brittle transition, T_{DB}, as a function of particle diameter d and volume fraction Φ for polyamide-6 systems. Symbols (◆, ●) show experimental data from ref 9: series **(a)** is obtained at fixed volume fraction $\Phi = 26\%$, and series **(b)** is obtained at fixed particle size $d = 300$ nm. Full lines represent model predictions for a typical Eyring description of σ_Y with $Y_0 = 110$ MPa, $Y_1 = 0.56$ Pa/°C, and $\sigma_B = 300$ MPa. Fitting parameters are **(a)** $C = 0.15$ and $\xi^* = 100$ nm and **(b)** $C = 0.26$ and $\xi^* = 10$ nm. Dotted lines show model predictions obtained by adjusting $\sigma_Y(T)$ to account for crystalline orientation effects. Fitting parameters are **(a)** $Y_0 = 76$ MPa, $Y_1 = 0.4$ MPa/°C, $C = 0.12$, and $\xi^* = 50$ nm and **(b)** $Y_0 = 48$ MPa, $Y_1 = 0.6$ MPa/°C, $C = 0.12$, and $\xi^* = 10$ nm.

the addition of particles has been shown to affect significantly the local flows during injection molding and to accentuate the crystalline orientation of the matrix with the chains axis parallel to the injection direction of impact test bars.[18] As a consequence, σ_Y and thus T_{DB} are expected to decrease as the matrix is more confined. We examine this effect by adjusting Y_0 and Y_1 to fit the data points that are likely to exhibit a strong matrix orientation, i.e., smaller particle sizes (Figure 5a) and higher volume fractions (Figure 5b). These new predictions are shown by dotted lines in Figure 5. The values obtained for Y_0 (∼50−70 MPa) and Y_1 (∼0.4−0.6 MPa/°C) are closer to the yield stresses measured in highly oriented polyamide-6.[1] Accordingly, experimental data deviate from model predictions toward higher T_{DB} for the larger particle sizes or lower volume fractions, which should correspond to less oriented matrices.

Other temperature effects could be introduced that complete our description of toughening. In particular, the glass transition of the semicrystalline matrix strongly affects chain mobility in the amorphous regions and leads to a change in the temperature dependence of σ_Y. This effect may be of particular interest in polyamides and some polyolefins for which the glass transition temperature is close to the temperatures of use ($T_{gPA} \sim 40$ °C, $T_{gPP} \sim -10$ °C). At very low temperature or very high impact speed, the glass transition of rubber also comes into play as it can significantly inhibits the cavitation of rubber filler. As a result, one would expect a cutoff in T_{DB} for temperatures lower than T_g of rubber.

More generally, eq 7 relates explicitly T_{DB} to the matrix and dispersion characteristics. This points at possible ways to repel the ductile-to-brittle transition toward even lower temperatures. A first trivial way is the use of plasticizers which favor chain mobility and thus lower σ_Y. A second way consists in tuning

ξ^* and σ_B to hinder crack opening and coalescence. This latter approach implies a control of the crystalline orientation and of the molecular organization within amorphous regions. Indeed, the crack size and the brittle stress have been shown to depend strongly on the degree of crystalline orientation and on the density in tie chains bridging crystalline lamellae.[21] In this regard, a proper design of the processing conditions (flows, cooling, and shear rates) and the addition of nucleating seeds or high molecular weight chains are certainly promising solutions.[31−33]

Conclusion

In conclusion, we show that a description of fracture in heterogeneous media explains the existence of a critical confinement length governing toughening of semicrystalline polymers. The proposed model predicts how this critical ligament thickness L_c depends on the matrix properties, particle size, and impact temperature. These predictions, together with the control and understanding of processing effects, bring new practical and quantitative guides for the design of super-tough materials. Furthermore, we believe that this picture extends beyond just semicrystalline polymers. It could help understanding the toughness of other complex heterogeneous structures such as polymer composites and biomaterials, the fracture of which often involves both localized cracking and dissipative molecular yielding. More generally, the present analysis shows that toughening is efficient if particles can initiate matrix yielding and bring confinement below the characteristic length scale of matrix heterogeneity. This may explain why toughening is much more difficult to achieve in the case of glassy polymer matrices where shear yield stresses are large and heterogeneities are at the nanometer scale. Accordingly, other toughening strategies are traditionally envisaged for glassy matrices, either by adding particles to perform crack arrest and multiple crazing or by modifying the molecular architecture of the polymer chain as it is done with block copolymers.

Acknowledgment. We thank A. D. Hollingsworth (NYU) for revision of the manuscript. Financial support from CNRS, ESPCI, and Arkema is gratefully acknowledged.

References and Notes

(1) Lin, L.; Argon, A. S. *J. Mater. Sci.* **1994**, *29*, 294.
(2) Donald, A. M.; Kramer, E. J. *J. Mater. Sci.* **1982**, *17*, 1765.
(3) Yee, A. F.; Pearson, R. A. *J. Mater. Sci.* **1986**, *21*, 2462.
(4) Bucknall, C. B.; Heather, P. S.; Lazzeri, A. J. *J. Mater. Sci.* **1989**, *16*, 2255.
(5) Argon, A. S.; Cohen, R. E. *Polymer* **2003**, *44*, 6013.
(6) Ahn, Y. C.; Paul, D. R. *Polymer* **2006**, *47*, 2830.
(7) Corté, L.; Rebizant, V.; Hochstetter, G.; Tournilhac, F.; Leibler, L. *Macromolecules* **2006**, *39*, 9365.
(8) Farquhar, T.; Zhao, Y. *Am. J. Bot.* **2006**, *93*, 1449.
(9) Borggreve, R. J. M.; Gaymans, R. J.; Schuijer, J.; Ingen Housz, J. F. *Polymer* **1987**, *28*, 1489.
(10) Wu, X.; Zhu, X.; Qi, Z. *Proc. 8th Int. Conf. Deform., Yield Fract. Polym.* **1991**, *78*.
(11) Bartczak, Z.; Argon, A. S.; Cohen, R. E.; Weinberg, M. *Polymer* **1999**, *40*, 2331.
(12) Loyens, W.; Groenickx, G. *Polymer* **2002**, *43*, 5679.
(13) Wu, S. *Polymer* **1985**, *26*, 1855.
(14) Corté, L.; Beaume, F.; Leibler, L. *Polymer* **2005**, *46*, 2748.
(15) Hobbs, S. Y.; Bopp, R. C.; Watkins, V. H. *Polym. Eng. Sci.* **1983**, *23*, 380.
(16) Margolina, A.; Wu, S. *Polymer* **1988**, *29*, 2170.
(17) Muratoglu, O. K.; Argon, A. S.; Cohen, R. E.; Weinberg, M. *Polymer* **1995**, *36*, 921.
(18) Schrauwen, B. A. G.; Govaert, L. E.; Peters, G. W. M.; Meijer, H. E. H. *Macromol. Symp.* **2002**, *185*, 89.
(19) Griffith, A. A. *Philos. Trans. R. Soc. London, Ser. A* **1920**, *221*, 163.
(20) Bouchaud, E. *Surf. Rev. Lett.* **2003**, *10*, 797.
(21) Kuksenko, V. S.; Tamuzs, V. P. In *Fracture Micromechanics of Polymer Materials*; Sih, G. C., Ed.; Martinus Nijhoff Publishers: Boston, 1981; pp 61−163.
(22) Broberg, K. B. In *Cracks and Fracture*; Academic Press: Cambridge, 1999.
(23) Seguela, R. *J. Polym. Sci., Part B* **2005**, *43*, 1729.
(24) Ward, I. M.; Hadley, D. W. In *Mechanical Properties of Solid Polymers*; Wiley: New York, 1993.
(25) Bowden, P. B.; Young, R. J. *J. Mater. Sci.* **1974**, *9*, 2034.
(26) Eudier, M. *Powder Metall.* **1962**, *5*, 278.
(27) Corté, L. Thesis, Université Pierre et Marie Curie, Paris, 2006.
(28) Vincent, P. I. *Plastics* **1964**, *29*, 179.
(29) Kohan, M. I. In *Nylon Plastics Handbook*; Hanser: Munich, 1995.
(30) Schrauwen, B. A. G.; v. Breemen, L. C. A.; Spoelstra, A. B.; Govaert, L. E.; Peters, G. W. M.; Meijer, H. E. H. *Macromolecules* **2004**, *37*, 8618.
(31) Galeski, A. *Prog. Polym. Sci.* **2003**, *28*, 1643.
(32) Kumaraswamy, G.; Verma, R. K.; Kornfield, J. A.; Yeh, F. J.; Hsiao, B. S. *Macromolecules* **2004**, *37*, 9005.
(33) Kumaraswamy, G. *J. Macromol. Sci., Polym. Rev.* **2005**, *45*, 375.

MA0706935